Start up and control of a DFIG wind turbine test rig

J.A. Cortajarena, J. De Marcos
EUITI
UPV-EHU
EIBAR, SPAIN
Email: josean.cortajarena@ehu.es

P. Alvarez, F.J.Vicandi, P.Alkorta
EUITI
UPV-EHU
EIBAR, SPAIN

***Abstract*— Power generated from wind is a fast growing renewable source of the world energy consumption. A test bench for comprehensive research on the doubly fed induction generator (DFIG) used as wind turbine is implemented. The wind energy is emulated with a synchronous machine according to the wind profile specified in the computer. Two inverters in a back to back configuration between the rotor and the grid are used to control the DFIG. The space vector pulse width modulation (SVPWM) technique is used in both inverters. Special attention has been placed in the offset adjustment of the encoder and the stator synchronization and connection to the grid. Finally, the regulation of the DFIG is performed controlling the active and reactive power to their reference values.**

I. INTRODUCTION

Wind power is gradually becoming a more significant part of worldwide electrical generation with significant engineering challenges for its assimilation and operation within mature transmission networks [1].

Doubly fed induction generator (DFIG) is the most commonly used type of generator in contemporary large variable speed wind turbines. This type of generator provides access to the rotor windings, giving the possibility of impressing a rotor voltage. In this way, power can be extracted or impressed to the rotor circuit and the generator can be magnetized from the stator or rotor circuit.

The main reason for the use of the doubly fed induction generator is that electronic equipment has to handle only a fraction of about 30% of the total system power. This means that the losses in the power electronic equipment are lower than in a directly connected full-power-rated converter topology. Cost saving of using a smaller converter is an important reason too [2].

The field oriented control (FOC) technique is used to control the DFIG, enabling the decoupled control of active and reactive power outputs [3]-[9].

This paper presents a complete implemented doubly fed induction generator wind turbine test rig. Some important aspects, like encoder offset detection to get the right rotor position and stator-grid synchronization to make a soft connection are implemented and tested. The starting up process of the test rig is fully automated. Stator, rotor and grid side converter currents, the DC link and grid voltages and the DFIG speed are measured for control purpose and to protect the system from undesirable high values.

Grid and rotor side converters in a back-to-back configuration (known as Scherbius drive) [10] control strategies are detailed. Also the wind power emulation and pitch control according to the selected wind speed reference and obtained power is explained.

Finally, experimental results are presented to validate the previously mentioned encoder offset determination, stator-grid synchronization and control.

II. TEST RIG

Figure 1 shows the schematic construction of the test rig with a 7.5 kW doubly-fed induction machine and an AC synchronous machine working as wind turbine emulator. The sensors to measure the currents and voltages are adapted and connected to the DS1003 control system from dSpace [11]. The impulses to control the rotor and grid side converters are generated by the DS1003. The rotor speed is measured with a 4096 impulse encoder via a FPGA connected to the DS1103 using the multiple period method [12].

A resistor, Rch, was included in series with the DC link connection (with a bypass circuit) to limit the inrush current when precharging the DC link. After a 10s delay, the resistors were bypassed by the PLC closing K5.

The DC Bus is charged before connecting the DFIG to the grid closing K4, and the connection of the system to the grid is done through K1, K2 and K3. By this scheme, the DFIG can be operated as a generator at a sub-synchronous and super-synchronous speed and the speed range depends on the power converters ratings and the machine mechanical limits.

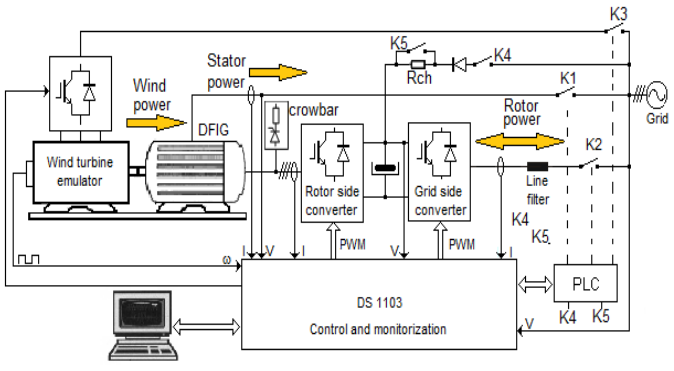

Fig.1. Doubly fed induction generator test rig.

TABLE I
RATINGS AND PARAMETERS OF DFIG (LEROY SOMER)

Stator Voltage 380V	J = 0.038Kg*m^2
Rotor Voltage 190V	P = 2 pole-pairs
Rated stator current 18A	Rr = 0.275Ω Rs = 0.325Ω Lm = 0.0664H
Rated rotor current 32A	Lls=0.00264H Llr=0.00372H
Rated speed 1447r.p.m.	Rated Torque 50Nm

TABLE II
RATINGS OF WIND TURBINE EMULATOR (CONTROL TECHNIQUES)

Stator Voltage 380V	Rated current 24.5 A
Rated Torque 50.4Nm	Rated speed 2000r.p.m.
Max. speed 3200r.p.m	Poles 8
Ke = 147V/krpm	Kt = 2.4Nm/A

DFIG and wind turbine emulator motor main characteristics are detailed in table I an II. The both converters are NFS-200 with IGBTs from Mitsubishi manufactured by Montelec, S.L. They can manage 75A to 7 kHz of switching frequency. The line filter is composed of 3 inductances of 2 mH @ 15A. A 4096-line optical encoder on the rotor shaft provides detailed rotor position and speed information.

III. ROTOR SIDE CONVERTER CONTROL EQUATIONS AND REFERENCE SYSTEM

The following equations describe the behavior of the doubly fed induction generator in a rotating reference frame oriented along the stator flux [3] [4] as depicted in figure 2.

$$\bar{v}_{s,dq} = R_s \bar{i}_{s,dq} + \frac{d\bar{\psi}_{s,dq}}{dt} + j\omega_e \bar{\psi}_{s,dq} \tag{1}$$

$$\bar{v}_{r,dq} = R_r \bar{i}_{r,dq} + \frac{d\bar{\psi}_{r,dq}}{dt} + j(\omega_e - \omega_r)\bar{\psi}_{r,dq} \tag{2}$$

$$\bar{\psi}_{s,dq} = L_s \bar{i}_{s,dq} + L_m \bar{i}_{r,dq} \quad \text{and} \quad L_s = L_m + L_{ls} \tag{3}$$

$$\bar{\psi}_{r,dq} = L_r \bar{i}_{r,dq} + L_m \bar{i}_{s,dq} \quad \text{and} \quad L_r = L_m + L_{lr} \tag{4}$$

$$T_e = \frac{3}{2} P\left(\psi_{sd} I_{sq} - \psi_{sq} I_{sd}\right) \tag{5}$$

$$T_e - T_L = J\frac{d\omega_m}{dt} + B\omega_m \tag{6}$$

$$P_s = \frac{3}{2}\left(v_{sd} i_{sd} + v_{sq} i_{sq}\right) \quad \text{and} \quad Q_s = \frac{3}{2}\left(v_{sq} i_{sd} - v_{sd} i_{sq}\right) \tag{7}$$

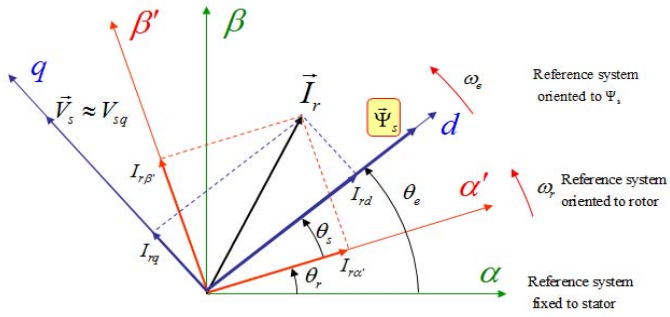

Fig.2. Reference systems used in the control of the DFIG.

where dq are the axis of the stator flux reference system.

$\bar{v}_{s,dq}$, $\bar{i}_{s,dq}$, $\bar{\psi}_{s,dq}$ are the stator voltage, current and flux vectors.

$\bar{v}_{r,dq}$, $\bar{i}_{r,dq}$, $\bar{\psi}_{r,dq}$ are the rotor voltage, current and flux vectors.

ω_r, ω_e, ω_m are the rotor electrical speed, stator flux reference system speed, and rotor mechanical speed.

L_m, L_s, L_r are the mutual, stator and rotor inductances.

L_{ls}, L_{lr} are the stator and rotor leakage inductances.

R_s, R_r are the stator and rotor resistances.

T_e, T_L are the motor and load torque.

J, B are the inertia of the system and friction coefficient.

P_s, Q_s are the stator active and reactive power

As can be seen in figure 2, the stator flux q component is 0, and when operating with equation 3 the next two equations are obtained,

$$i_{sd} = \frac{|\bar{\psi}_s|}{L_s} - \frac{L_m}{L_s} i_{rd} \tag{8}$$

$$i_{sq} = -\frac{L_m}{L_s} i_{rq} \tag{9}$$

This means that the stator current can be controlled with the rotor current. Taking into account that the stator resistance is small, the stator flux can be considered constant and its value is,

$$|\bar{\psi}_s| \approx \frac{|\bar{V}_s|}{\omega_e} \tag{10}$$

The stator voltage d component is almost zero because the reference system is oriented along the stator flux, so it can be obtained that,

$$P_s \approx -\frac{3}{2}\omega_e \Psi_s \frac{L_m}{L_s} i_{rq} \tag{11}$$

$$Q_s \approx \frac{3}{2}|V_s|\left[\frac{|V_s|}{\omega_e L_s} - \frac{L_m}{L_s} i_{rd}\right] \tag{12}$$

Equations 11 and 12 show that the stator active power is controlled with the q component of the rotor current and the stator reactive power with the rotor current d component.

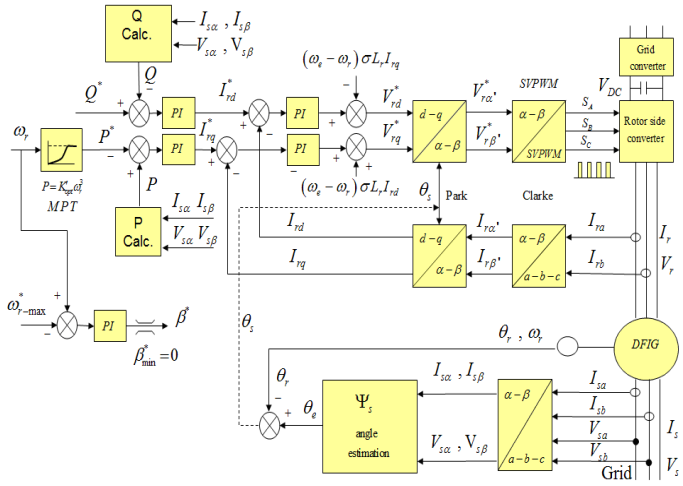

Fig.3. DFIG control structure.

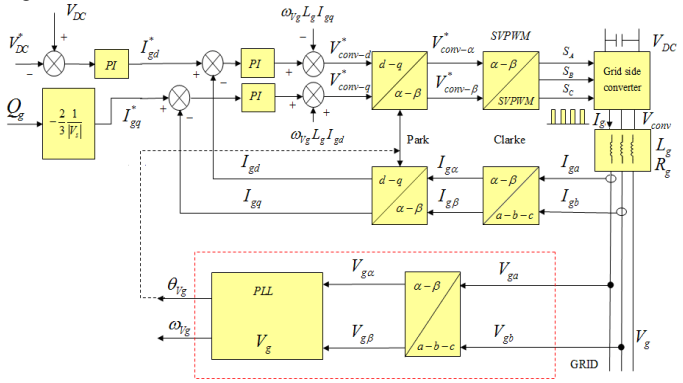

Fig.4. Grid side converter control structure.

Figure 3 shows the block diagram for the control of the DFIG from the rotor side. The errors between measured active and reactive power and reference values are fed into PI controllers giving the current references I^*_{rq} and I^*_{rd} respectively. These current references are compared to the actual currents and the errors are the inputs of another two PI controllers, getting at their outputs the rotor voltage references V^*_{rq} and V^*_{rd}. Finally the converter impulses S_A, S_B, S_C are obtained.

IV. Grid Side Converter Control Equations and Reference System

The following equations describe the behavior of the grid side converter connected to the grid trough a line filter Lg and Rg as shown in figure 4.

$$\overline{v}_{conv,dq} = R_g \overline{i}_{g,dq} + L_g \frac{d\overline{i}_{g,dq}}{dt} + \overline{v}_{g,dq} \tag{13}$$

$$P_g = \frac{3}{2}\left(v_{gd} i_{gd} + v_{gq} i_{gq}\right) \quad \text{and} \quad Q_g = \frac{3}{2}\left(v_{gq} i_{gd} - v_{gd} i_{gq}\right) \tag{14}$$

where $\overline{v}_{conv,dq}$, $\overline{i}_{g,dq}$, $\overline{v}_{g,dq}$ are the grid side converter output voltage, grid current and grid voltage respectively.

R_g , L_g are the grid line filter resistance and inductance.

To control the grid side converter, the rotating reference axis d-q will be oriented along the grid voltage, angle θ_{Vg}. Thus, the grid voltage q component is 0 and the active power is regulated with the grid current d component. The reactive power is regulated with the grid current q component,

$$P_g = \frac{3}{2} v_{gd} i_{gd} \quad \text{and} \quad Q_g = -\frac{3}{2} v_{gd} i_{gq} \tag{15}$$

Figure 4 illustrates a block diagram of the implemented grid side controller. The measured dc-link voltage is compared to the dc-link voltage reference and the error is fed into a PI controller to get at their output the active current reference I^*_{gd}.

I^*_{gd} is compared with the real I_{gd} current and the error is the input of the PI to get to their output $V^*_{conv\text{-}d}$. The $V^*_{conv\text{-}q}$ is obtained from the reactive power control.

V. Wind Profile and Pitch Regulation

Wind turbines are designed to yield maximum electrical power at wind speeds around 12 meters per second. In the case of stronger winds it is necessary to waste part of the wind energy avoiding a damage of the generator.

The wind turbine emulator will give a mechanical power to the DFIG according to the preset wind speed in the computer. If the emulated wind power exceeds the maximum power of the DFIG, pitch control emulation will limit the obtained power from the wind emulator [6] [7].

The power transmitted to the hub of a wind turbine can be expressed as,

$$P_{turb} = \frac{1}{2} C_p(\lambda, \beta) \rho_{air} \pi R^2 {v_w}^3 \tag{16}$$

Where ρ_{air}, is the mass density of the air, R is the radius of the propeller, Cp is the power performance coefficient, v_w is the wind speed, β is the pitch angle and λ is the blade tip speed ratio and is defined as,

$$\lambda = \frac{R \cdot \omega_{pr}}{v_w} \tag{17}$$

and ω_{pr} is the angular velocity of the propeller.

The power performance coefficient Cp, used according to the tip speed ratio and the pitch angle is shown in figure 5.

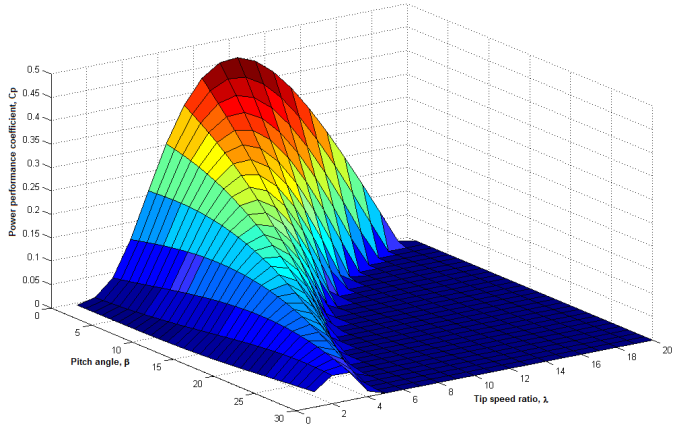

Fig.5. Power coefficient versus pitch angle and tip speed ratio.

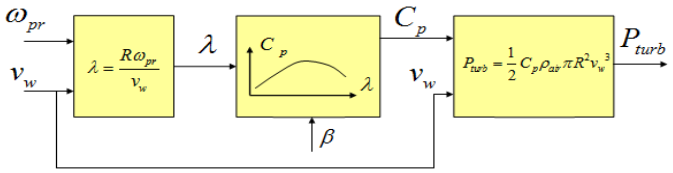

Fig.6. Turbine power reference according Cp, ω_{pr} , and v_w.

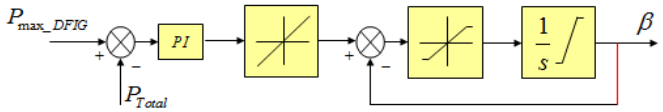

Fig.7. Pitch angle control structure.

Structure of figure 6 is used to get the turbine power reference, allowing to study the obtainable power depending on the Cp working point. Different MPT [5] (maximum power tracking) strategies can be tested. The pitch angle is controlled with the structure of figure 7 when the measured total power injected to the grid, P_{Total}, exceeds the maximum DFIG power.

VI. Encoder Offset and DFIG Connection to Grid

The connection sequence of the DFIG to the grid begins with the charging of rotor and grid converters DC bus. Once this DC bus is charged and if the grid side reference system is oriented with the grid voltage the grid side converter is connected trough contactor K2 and regulation of DC bus to a fixed value will begins.

The grid connection process of the DFIG starts when the machine speed reaches the minimum operating value, fixed for the wind turbine emulator.

Before realizing the connection of the stator to the grid the DFIG is turning and two steps have to be done previously. The first one is the detection of the encoder offset respecting the stator flux, and the second step is the synchronization of the stator voltage with the grid voltage.

Once all the steps are finished, the stator will be connected to the grid trough contactor K1 and the regulation of active and reactive power will begin.

The rotor angle is necessary to realize the control with the rotor currents in the stator flux reference system as mentioned before. If the stator circuit is open, that is, stator current is zero, equations 3 and 4 become,

$$\bar{\psi}_{s,dq} = L_m \bar{i}_{r,dq} \quad \text{and} \quad \bar{\psi}_{r,dq} = L_r \bar{i}_{r,dq} \tag{18}$$

Both equations show that the stator flux and the rotor flux are in phase, it doesn't care in which reference system, because both are created by the same current. So, to get the right position of the rotor angle with the encoder, the rotor is excited with a fixed current, lower than rated value, and the stator is open and there isn't stator current. The stator flux is obtained from the voltage model, in the reference system fixed to the stator and the rotor flux is obtained from the current model in the rotor oriented reference system, see figure 8.

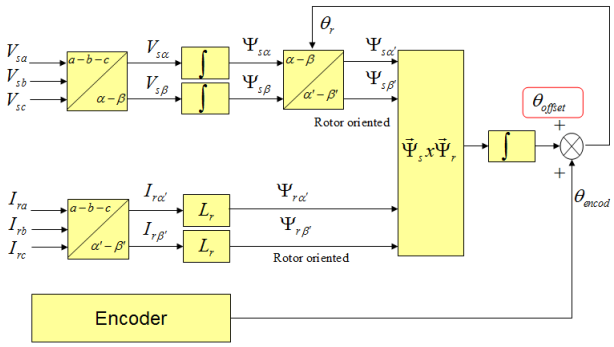

Fig.8. Encoder offset determination structure.

The stator flux is transformed into the rotor reference system with the rotor angle adapted by an integrator. When both fluxes are equal the encoder offset is captured.

Once the rotor angle is obtained correctly with the encoder, the stator-grid synchronization will start. Stator and grid will be synchronized when stator voltage and grid voltage are of the same amplitude and they are in phase. The way to do this is keeping the stator circuit open, and regulating the stator voltage from the rotor side.

Operating with equations 1 and 3, with stator current equal zero and working at steady-state, this is d/dt = 0,

$$\bar{v}_{s,dq} = R_s \bar{i}_{s,dq} + \frac{d\left(L_s \bar{i}_{s,dq} + L_m \bar{i}_{r,dq}\right)}{dt} + j\omega_e \left(L_s \bar{i}_{s,dq} + L_m \bar{i}_{r,dq}\right) \tag{19}$$

$$\bar{v}_{s,dq}\Big|_{\bar{i}_{s=0} \;\&\; steady} = j\omega_e L_m \bar{i}_{r,dq}$$

so,

$$v_{sd} = -\omega_e L_m i_{rq} \tag{20}$$

$$v_{sq} = \omega_e L_m i_{rd} \tag{21}$$

These equations show that stator voltage will be adjusted with the rotor current, and the synchronization structure it is shown in figure 9. The rotor current d and q components are adjusted by two PI regulators to get the grid and stator voltage in phase and of the same amplitude.

Once the synchronization is achieved, the stator could be connected to the grid. At this moment, the rotor current d and q references are changed to the active and reactive power controllers output. To have a soft transition between the connection moment and the power regulation, the PI integral terms of the synchronization moment are loaded into the PI rotor current regulators.

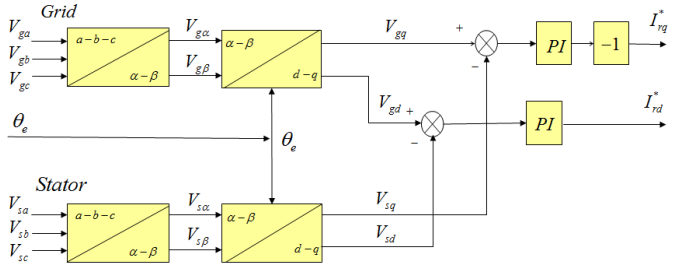

Fig.9. DFIG stator-grid synchronization structure.

VII. EXPERIMENTAL RESULTS

Simulations were done before starting with the experimental tests to validate all the mentioned control structures. In this paper, only the obtained results from the experimental tests with the implemented test rig are shown.

Figure 10 shows the encoder offset detection. The DFIG rotor is running moved for the wind turbine emulator at low speed and the grid side converter is already regulating the DC link voltage. The offset detection process begins regulating the rotor current to 6A. Initially the rotor and stator flux are out of phase but the encoder offset determination structure is adjusting the encoder offset, bottom of figure 10, and both fluxes become in phase in a short period of time. When the phase error is very close to zero the offset is captured to correct the encoder angle.

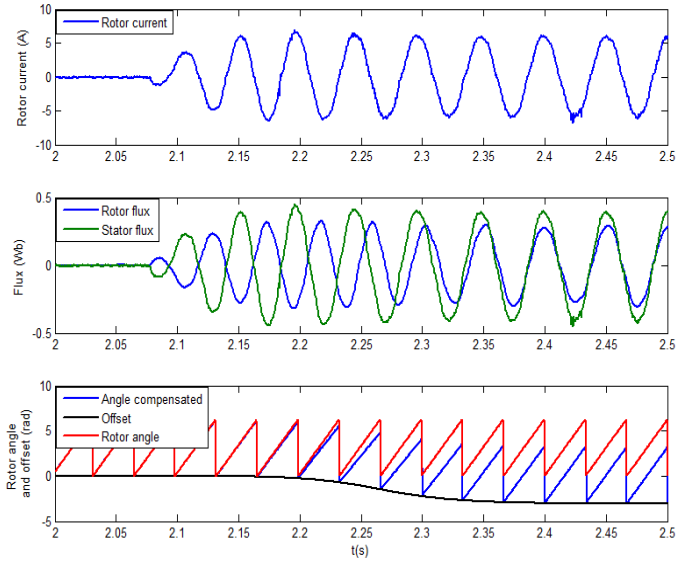

Fig.10. Encoder offset determination. Top, one phase rotor current. Medium, rotor and stator flux. Bottom, encoder angle ,offset and angle compensated.

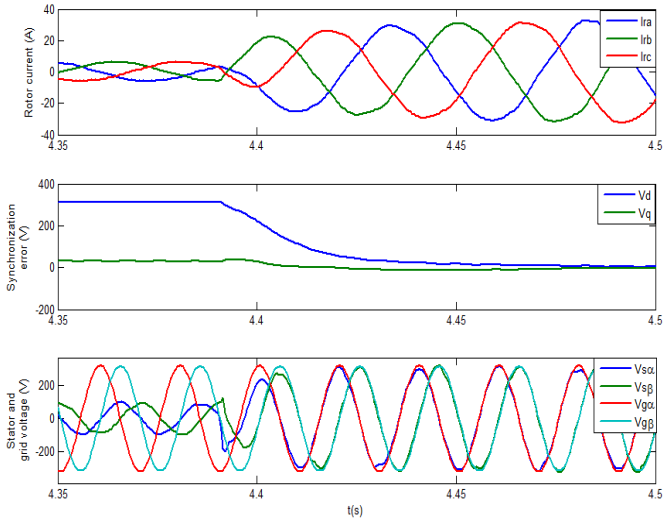

Fig.11. Stator-grid synchronization. Top, rotor current. Medium, stator-grid voltage error. Bottom, stator and grid voltages.

Stator-grid synchronization signals can be seen in figure 11, and the structure of figure 9 is used. After finishing the encoder offset determination, the stator-grid synchronization begins. This happens at instant 4.39s, when the rotor current changes because the rotor current d and q references are generated by the PI regulators. The d and q voltage error decreases at the time that the stator voltage and grid voltage are getting equal. When the voltage error in axes d and q are very close to zero, the synchronization is finished and connection of stator to grid is done.

Figure 12 shows the stator-grid connection moment. Before the connection, stator and grid voltage are almost equal. At the connection moment rotor current is no changing and stator current increases according to the power that is getting the DFIG from the wind emulator.

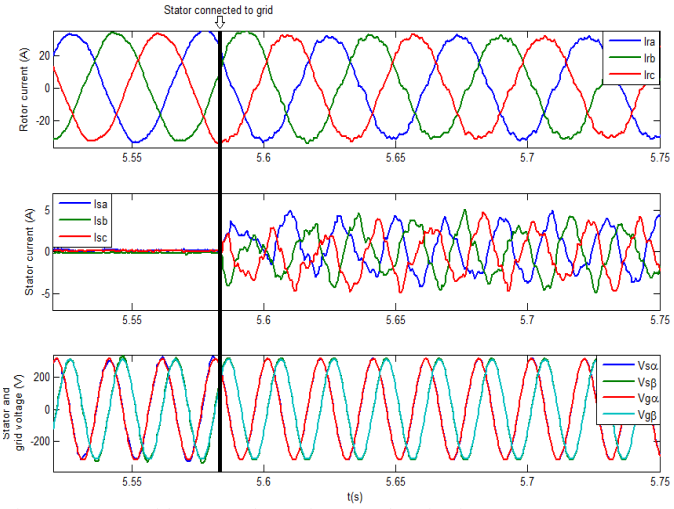

Fig.12. Stator-grid connection after synchronization. Top, rotor current. Medium, stator current. Bottom, stator and grid voltages.

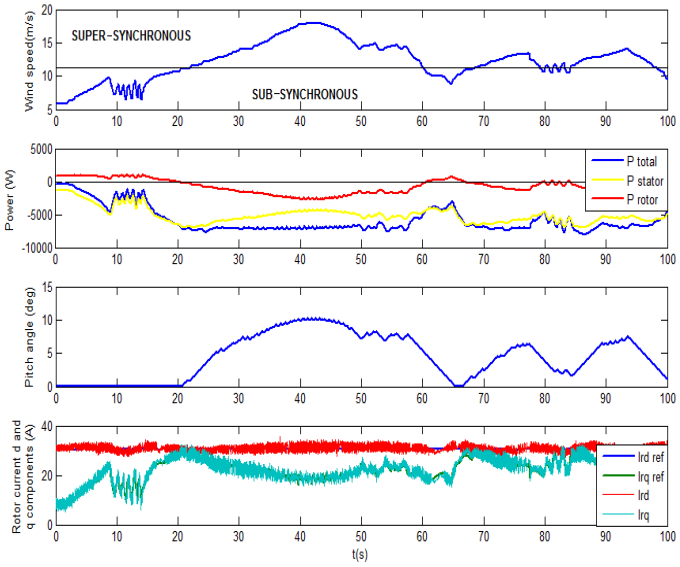

Fig.13. Wind speed changing. Top, wind speed profile. Second, stator, rotor and total power. Third, pitch angle. Bottom, rotor current d and q components.

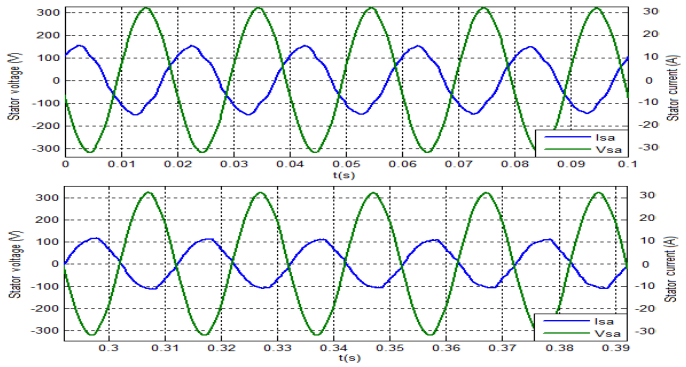

Fig.14. Stator voltage and current for two different P and Q reference values.

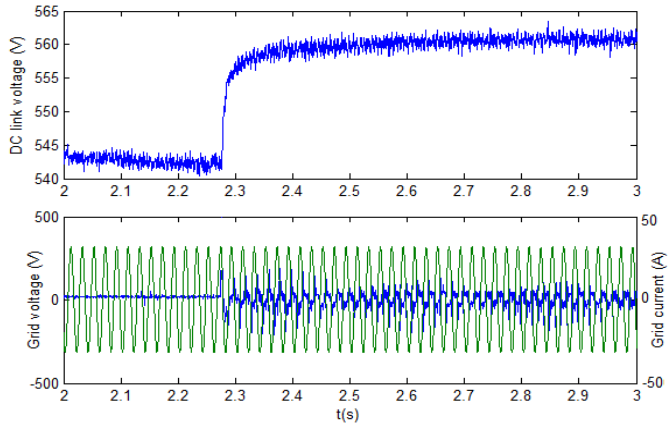

Fig.15. Top, DC link voltage regulation. Bottom, grid voltage and current of grid side converter.

Figure 13 shows the regulation of the DFIG when the wind speed is changing. The wind speed is changing from 6m/s to 18m/s, that means a rotor speed from 900 to 2800 rpm. For a speed higher than 12m/s the DFIG is working in super-synchronous mode and in sub-synchronous mode when speed is lower than 12m/s. The energy from the stator is flowing always towards the grid. Energy through the rotor changes of direction as function of the rotor speed. At speeds lower than synchronous the rotor energy is absorbed from the grid and is going from rotor towards stator. For this reason, the total power is lower than the stator power. When the speed is higher than synchronous, the rotor energy changes the direction and it is going from rotor towards grid. When the total power is higher than 7kW and the speed is increasing the pitch regulation changes the pitch angle limiting the maximum power. The rotor current d component is constant because there is not change in the reactive power reference. Instead, the rotor q component is changing because the power changes according to the wind speed.

Figure 14 shows one phase stator voltage and current for different values of active and reactive power reference. The top graph P reference is 5.4kW and the Q reference is 4.2kVAR. The bottom graph P reference is 5.4kW and the Q reference is 0VAR.

Figure 15 shows the start time of the DC link regulation to 560V and the grid side voltage and current at that moment.

VIII. CONCLUSION

In this paper, the details for the implementation of a wind turbine test rig based on a DFIG were proposed. A wind turbine emulator is configured to produce the wind power. The details for the encoder offset determination, stator-grid synchronization for a soft stator connection to the grid and the system regulation including a pitch control were implemented and tested in DS1003 platform. The results obtained show a good performance of the implemented test rig. The starting up process of the test rig turns out to be very safe because is fully automated. References like wind speed, reactive power, DC link voltage value, etc, can be changed very easily and visualization of any signal of the system becomes very simple.

ACKNOWLEDGMENT

The authors wish to thank to the Proyectos de Investigación Focalizada Bizkaia 2008, project with ref. DIPE08/20 and SAIOTEK (ORAV) with ref. S-PE09UN12 for their support of this research.

REFERENCES

[1] S. Krohn, Ed., "The Economics of Wind Energy." Belgium: European Wind Energy Association (EWEA), Mar. 2009.

[2] A. D. Hansen, F. Iov, F. Blaabjerg, and L. H. Hansen, "Review of contemporary wind turbine concepts and their market penetration," J. Wind Eng., vol. 28, no. 3, pp. 247–263, 2004.

[3] G. Pannell, D. J. Atkinson, and B. Zahawi, "Analytical Study of Grid-Fault Response of Wind Turbine Doubly Fed Induction Generator." IEEE Transactions on Energy Conversion, VOL. 25, NO. 4, December 2010.

[4] N. P. Quang, A. Dittrich, A. Thieme "Doubly-fed induction machine as generator: control algorithms with decoupling of torque and power factor". Electrical Engineering 80(1997)325-335, Springer-Verlag 1997.

[5] S. Bhowmik, R. Spee, and J. H. R. Enslin, "Performance Optimization for Doubly Fed Wind Power Generation Systems" IEEE Transactions on Industry Applications, VOL. 35, NO. 4, July/August 1999.

[6] E. Muljadi, and C. P. Butterfield. "Pitch-Controlled Variable-Speed Wind Turbine Generation". IEEE Transactions on Industry Applications, VOL. 37, NO. 1, January/February 2001.

[7] M.A. Pöller, "Doubly-Fed Induction Machine Models for Stability Assessment of Wind Farms", in Proc. IEEE PowerTech, Bologna, Italy, June, 2003, BPT0-345.

[8] A. Mullane, M. O´Malley, "The Inertial Response of Induction-Machine-Based Wind Turbines", IEEE Trans. Power Systems, vol. 20, pp. 1496-1503, Aug. 2005.

[9] R. Pena, R. Cardenas, E. Escobar, J. Clare, P. Wheeler."Control strategy for a Doubly-Fed Induction Generator feeding an unbalanced grid or stand-alone load" Electric Power Systems Research 79 (2009) 355–364

[10] S. Gallardo, J.M. Carrasco, E. Galván, L.G. Franquelo. "DSP-based doubly fed induction generator test bench using a back-to-back PWM converter".The 30th Annual Conference of the IEEE Industrial Electronics Society, November 2 - 6, 2004, Busan, Korea

[11] dSPACE, "Real –Time Interface. Implementattion Guide.Experiment Guide. For Realese 5.0" GmbH Paderborn, Germany 2005.

[12] J.A. Cortajarena, J.De Marcos, P. Alkorta, F.J.Vicandi P. Alvarez "System to study induction motor speed estimators" SAAEI06,Gijón, September 2006